Received: January 13, 2021. Revised: April 2, 2021. 468

International Journal of
Intelligent Engineering & Systems

http://www.inass.org/

Adaptive Power System Stabilizer Using Kernel Extreme Learning Machine

IBG Manuaba[1] Muhammad Abdillah[2] Ramon Zamora[3] Herlambang Setiadi[4]*

[1]*Department of Electrical Engineering, Universitas Udayana, Indonesia*
[2]*Department of Electrical Engineering, Universitas Pertamina, Indonesia*
[3]*Department of Electrical Engineering, Auckland University of Technology, New Zealand*
[4]*Faculty of Advanced Technology and Multidicipline, Universitas Airlangga, Surabaya, Indonesia*
* Corresponding author's Email: h.setiadi@stmm.unair.ac.id

Abstract: A disturbance such as a small load change in the electrical power grid triggers the system to oscillate and may lead to performance degradation of the control system in the generation source unit. To overcome this problem, a power system stabilizer (PSS) is added as a supplementary control in the power system grid to damp the oscillation caused by the disturbance. This paper proposes a kernel extreme learning machine (K-ELM) method to adjust the parameters of PSS for a wide range of operating conditions. The proposed control scheme in this research work is PSS based on K-ELM called KELM-PSS. To examine the robustness of KELM-PSS, a single machine infinite bus (SMIB) is utilized as a test system. The simulation results showed that the KELM-PSS provided a satisfactory result in both the training and testing phases. In the training process, KELM-PSS has a smaller mean square error (MSE) value, mean absolute error (MAE) value, and sum square error (SSE) value in terms of accuracy criterion compared to PSS based on machine learning such as extreme learning machine (ELM), support vector machine (SVM), and least square support vector machine (LS-SVM). Also, in terms of computation time, KELM-PSS has faster CPU time than other machine learning methods to obtain the parameters of PSS. The parameters of K-ELM including the regularization coefficient Cr and kernel parameter σ obtained from the training phase are utilized in the testing process. In a testing phase, the K-ELM approach will obtain the appropriate parameters of PSS (Kstab, T1, and T2) when there are changes of generator real power output P, reactive power output Q, terminal voltage Vt, and equivalent reactance Xe. In this stage, KELM-PSS could decrease the overshoot and compress the settling time better than other approaches utilized in this study. Moreover, KELM-PSS has the best performance index based on integral time absolute error (ITAE) compared to other techniques utilized in this research work.

Keywords: Power system stabilizer, Power system stability, Extreme machine learning, Kernel extreme machine learning, Support vector machine, Least square support vector machine.

1. Introduction

In an electric power system, stability is still being a worldwide issue that associates with the economic development of a country as well as people's subsistence [1, 2]. Therefore, it has always been great attention to power system researchers and engineers [3]. Stability is required to keep the electrical power secure and reliable [4, 5]. A stability problem in power system operation may be induced by either a small disturbance or a large disturbance [6]. A large disturbance is commonly triggered by a short circuit, transmission line outage, and generator outage. A small disturbance is produced by load change dynamically [7]. The term stability in an electric power system is defined as the ability of the electrical power system to maintain system synchronization [8-12]. In a stable operational state, all generators rotate at synchronous speed so that there is a balance between the mechanical input power on the prime mover and the electrical output power in the system. If the mechanical input power does not quickly adjust to match the load power, the rotor speed (in this case, the system frequency) and the voltage of the generator will deviate from normal conditions [13]. If a disturbance occurs, there is a difference value

between the mechanical input power and the electrical output power from the generator. This disturbance triggers the oscillation in the power system grid. Therefore, this oscillation should be damped to maintain the quality of electric power within a certain limit [14].

To improve the electrical power system stability, several approaches have been proposed and reported in the literatures such as automatic voltage regulator (AVR) [15]. In [15], the authors try to adjust the output of AVR to damp the oscillatory condition of power system. PIDA based on whale optimization is used as the proposed method to adjust the AVR output. Static series synchronous compensator (SSSC) is proposed by authors in [16] to enhance the dynamic stability of wind power system. It is found that the dynamic stability of wind power system can be enhanced by using SSSC. Research effort in [17], try to utilizer static var compensator (SVC) for handling the unstable condition of power system considering renewable energi integration. To make SVC more optimal fuzzy logic controller is added in SVC. It is found that fuzzy-SVC can enhance the stability of power system with wind power system. Gurung et all [18] proposed the application of power system stabilizer (PSS) to enhance small signal stability of power system considering uncertainty of renewable based power plant. Bat algorithm is used as optimization method for designing PSS. It is noticeable that PSS can handle the uncertainty power output impact in small signal stability. Research in [19], try to utilize thyristor control series capacitor (TCSC) to enhance the active and reactive power stability of power system. The application of unified power flow controller (UPFC) for enahncing the power system stability boundary is described in [20]. In [20], diffirent sizing and location may giving different results on system performance. Installing superconducting magnetic energy storage (SMES) is enhancing the dynamic stability performance of power system as investigated in [21]. Research effort in [22], is investigate the influence high voltage direct current (HVDC) installation in oscillatory stability performance. In [22], it is noticeable that HVDC installation give a positive impact on oscillatory stability. Furthermore, Research effort in [23, 24] shows that installing static synchronous compensator (STATCOM) and virtual synchronous generators (VSGS) [24] could enhance the power system stability performance.

Among the methods above, power system stabilizer (PSS) is widely utilized to damp the oscillation on the power system network. PSS is also cheaper compared to the other devices such as FACTS devices and energy storage devices. Moreover, it is difficult to obtain the appropriate parameters of conventional PSS by using the trial-error method. Furthermore, when the change of load value occurs, it will cause the problem such as the change of operation point of the power system. In this condition, the parameters of PSS should be adjusted to stabilize the system and take a long time when it is conducted by the trial-error approach. One of PSS types namely PSS2B has been applied worldwide to damp the oscillation of power system because it has a simple parameter and satisfactory control performance [25, 26]. Meanwhile, PSS2B has drawbacks when applied for small signal stability study because it has been restricted by the critical gain of the high-frequency band. PSS4B, another type of PSS, has been proposed to tackle the drawback of the PSS2B by introducing two variable inputs and multi-parallel branches. However, phase relationships and parameter tuning of PSS4B are really complicated to compute [27, 28]. Thus, this PSS is difficult to implement in engineering field. In order to increase the dynamic stability of power system network, some scenarios such as optimal placement, design, and parameter tuning of PSS have been researched, proposed, and reported in literatures. A saturated robust PSS has been proposed by taking into account the uncertainty [29, 30]. The advanced PSS based on adaptive control approach has also been designed [31, 32].

Nowadays, artificial intelligence technique has been widely utilized to solve hard engineering problem. To obtain the appropriate parameters of PSS under wide range of operating conditions, some approaches based on artificial intelligence methods have been utilized and reported in the literature such as adaptive fuzzy sliding mode controller (AFSMC) [33], backtracking search algorithm (BSA) [34], modified Nyquist diagram with an embedded partial pole-placement capability [35], genetic programming (GP) [36], cuckoo search optimization [37], hyper-spherical search (HSS) optimization algorithm [38], cross-gramian model reduction approach [39], bat algorithm [40], and particle swarm optimization (PSO) [41]. However, optimization based design have a drawback in handling operating condition fluctuation. PSS based optimization approach should tune their parameter everytime the operating condition of the system changing. Hence, it will take a lot of effort and time for the PSS to tune the parameter. Hence it is important to make PSS adaptive to operating condition fluctuation. To make PSS adaptive, kernel extreme learning machine (K-ELM) method can be used.

This paper proposes a method, namely the kernel extreme learning machine (K-ELM), as an extension

of the conventional extreme learning machine, to obtain the appropriate parameters of power system stabilizer adaptively to provide optimal damping settings to power system grid. To test the effectiveness of the proposed method, the optimization model uses a single machine infinitive bus (SMIB). The mean square error (MSE), mean absolute error (MAE), and sum square error (SSE) are employed to measure the accuracy of the proposed method during training phase of K-ELM. Furthermore, to examine the robustness of PSS based on K-ELM (KELM-PSS), integral time absolute error (ITAE) is considered. From the simulation results, the performance of the proposed method called KELM-PSS provides better damping for power system oscillation than the standard extreme learning machine (ELM), support vector machine (SVM), and least-square support vector machine (LS-SVM).

The rest of the paper is organized as follows. Power system model and proposed method are explained in Section 2. Implementation of proposed method is described in Section 3. Results and discussions are illustrated in Section 4. Conclusions are given in Section 5.

2. Power system model and proposed method

In this section, a brief overview of power system stabilizer, single machine infinite bus, and kernel extreme learning machine is provided. The notations utilized in this paper are provided in Table 1.

Table 1. List of notations used in this paper

Symbol		Meaning
A	:	State matrix
B	:	Control or input matrix
C	:	Output matrix
C_r	:	Regularization coefficient
D	:	Disturbance matrix
D_m	:	Mechanical damper
E_A	:	Sending bus
E_B	:	Receiving Bus
$e(t)$	:	The difference between the desired rotor speed value and the measured value of speed rotor deviation.
f_0	:	Frequency of SMIB system
H	:	Hidden layer output
H_m	:	Inertia constant
K_1, K_2, K_4, K_5, K_6	:	The functions of the operating real and reactive loading as well as the excitation levels in the generator
K_3	:	A function of ratio of impedance
K_A	:	Amplifier gain
K_E	:	Exciter gain
K_F	:	Filter gain
K_{gu}	:	Gain of governor
K_{stab}	:	PSS gain
N	:	Number of datasets
R_e	:	Equivalent resistance of transmission line
T	:	Predicted output
T_1, T_2	:	Time constant of phase compensation
T_A	:	Time constant of amplifier
T_E	:	Time constant of exciter
T_F	:	Time constant of filter
T_{gu}	:	Time constant of governor
T_r	:	Time constant of transducer
t_{sim}	:	The time simulation
T_{tu}	:	Time constant of turbine
T_w	:	Time constant for washout filter
T'_{do}	:	Time constant for generator field
X_e	:	Equivalent reactance of transmission line
$\hat{y}_i$	:	The predicted PSS parameters (i.e. K_{stab}, T_1, and T_2)
y_i	:	The real data record of PSS parameters (i.e. K_{stab}, T_1, and T_2)
Z_{eq}	:	Equivalent impedance
$h(x) = [h_1(x), h_2(x), \ldots, h_M(x)]$:	:	The output of hidden layer with respect to input x.
$\beta = [\beta_1, \beta_2, \ldots, \beta_M]$:	:	The output weights between the hidden layer of M neuron and output neuron
σ	:	Kernel parameter
$\Omega(x, y)$	:	The kernel function of hidden neurons of SLFN
$\Delta E'_q$	:	Voltage generator deviation
ΔP_c	:	Governor control
ΔP_L	:	Deviation of load or disturbance
ΔT_e	:	Electrical torque deviation
ΔT_G	:	Governor output deviation
ΔT_m	:	Mechanical torque deviation
ΔU	:	Input vector
ΔV_A	:	Voltage deviation of amplifier
ΔV_F	:	Voltage deviation of filter
ΔV_{FD}	:	Voltage field deviation
ΔV_{Le}	:	Voltage output of washout filter
ΔV_R	:	Transducer voltage deviation
ΔV_{REF}	:	Voltage reference
ΔV_s	:	Deviation of PSS output
ΔV_t	:	Terminal voltage of generator
ΔX	:	State vector
ΔY	:	Output vector
$\Delta\omega$	:	Rotor speed deviation
$\Delta\omega_B$	:	$2\pi f_0$

2.1 Power system stabilizer

To preserve the system stability caused by any type of disturbances, generators in the power system grid are equipped with PSS [42]. The aim of installing the PSS is to augment power system stability by damping out the oscillations by generating control signal via excitation system of the generators. Generally, PSS utilizes the phase compensation method to obtain its parameters in order to provide appropriate damping. A PSS is generally consisting of amplifier gain and lead-lag compensation element as depicted in Fig. 1. The transfer function of a conventional power system stabilizer with rotor speed deviation (Δω) considered as PSS input is defined in Eq. (1). This transfer function can be illustrated as the block diagram in Fig. 1.

$$\frac{\Delta V_s}{\Delta \omega} = K_{stab} \frac{sT_w}{1+sT_w} \frac{(1+sT_1)}{(1+sT_2)} \tag{1}$$

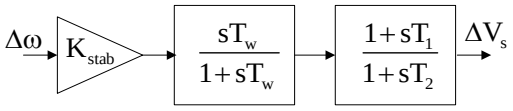

Figure. 1 Power system stabilizer representation

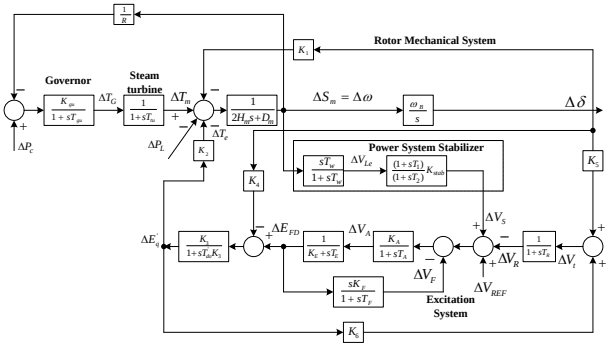

Figure. 2 Overall SMIB system block diagram with conventional PSS

2.2 Single machine infinite bus

The exciter which functions as the main control and regulator for frequency control generally complements the installed generator as shown in the Fig. 2. Generator control and excitation arrangements play an important role in increasing the dynamic stability of the power system. The infinite bus is a representation of the load bus which is usually a substitute for a large rigid system with a constant voltage and angle. Mathematical modeling of the system is the first step in analyzing and designing a control system. Furthermore, the general methods used are the transfer function approach and the state equation approach. For the use of transfer functions and linear state equations, the system must first be linearized.

One machine is connected to the infinite bus via a transmission line and is considered operating under different load conditions. The model is shown in Fig. 3. This simple dynamic model of a power system is called a single machine infinite bus (SMIB). The SMIB system, which is called a plant, consists of a synchronous generator connected via a step-up transformer and a parallel two-line transmission line which is an assumed very large power grid with unlimited buses. The synchronous generator itself is driven by a turbine with a governor and an exciter with an external excitation system. The excitation system is controlled by an automatic voltage regulator (AVR) and a power system stabilizer (PSS).

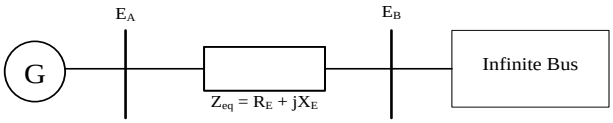

Figure. 3 Equivalent of single machine connected to a power system grid via a transmission line

The power system is a typical dynamic system with linearization at the output point so that the total linearization system model with AVR and PSS can be written in the following equations:

$$\frac{d\Delta X}{dt} = \mathrm{A}\Delta X + \mathrm{B}\Delta U \tag{2}$$

$$\frac{d\Delta X}{dt} = \mathrm{A}\Delta X + \mathrm{B}\Delta U \tag{3}$$

The complete system to be simulated contains three separate blocks: mechanical loop, electric loop and PSS. The state vector and input vector are defined as follows [41, 44]:

$$X = \begin{matrix}[\Delta\omega\ \Delta\delta\ \Delta T_m\ \Delta T_G\ \Delta E'_q\ \ \Delta V_{Le}{}^T \\ \Delta V_s\ \Delta V_{FD}\ \Delta V_F\ \ \Delta V_A\ \Delta V_R]\end{matrix} \tag{4}$$

$$U = [\Delta P_L\ \Delta P_C\ \Delta V_{ref}] \tag{5}$$

2.3 Kernel extreme leaning machine (KELM)

The basis of the structural model of the extreme learning machine (ELM) is a feed-forward neural network with a hidden layer as a single hidden layer of the feed-forward neural network (SLFN). ELM has extraordinary speed for mapping the correlation between input and output data. ELM uses learning

techniques to correct weaknesses of traditional neural networks (NN) and minimize empirical risk, namely minimizing training errors so that they are compatible with non-linear functions in input and output data sets. The weakness of the conventional neural networks usually requires a longer learning time due to repeated determination of network parameters and more training samples to get the output accurately. ELM does not require iteration so that ELM learning time is faster than standard neural networks. In addition, conventional neural networks usually require longer learning times because the network parameters are determined repeatedly, and more training samples are included to obtain predictive output accurately. ELM has a weakness, namely the calculation of hidden neurons using the trial-and-error (TEM) method and requires more neurons in the hidden layer for the randomly selected ELM weighting parameters. The kernel functions in ELM are used to map data from the hidden input layer into the higher dimensional feature subspace. Non-linear patterns become linear and computationally intensive operations can be avoided. The ELM learning algorithm is more flexible and stable because it does not require node parameters to be randomly selected from the hidden or input layers. The ELM algorithm was introduced by G.B. Huang in 2006 [43].

The mathematical model of the ELM output with the *M* data sample is defined as follows:

$$y_M(x) = \sum_{i=1}^{M} \beta_i h(x) \tag{6}$$

Minimizing training errors and output weights at the same time are the goals of the ELM learning algorithm as defined in Eq. (7).

minimize:

$$\|H\beta - T\|, \|\beta\|. \tag{7}$$

The least squares solution of (7) based on KKT conditions can be written as:

$$\beta = H^T \left(\frac{1}{C_r} + HH^T\right)^{-1} T \tag{8}$$

By substituting Eq. (8) into Eq. (6), the output of ELM can be obtained as defined in the following equation:

$$y(x) = h(x)H^T \left(\frac{1}{C_r} + HH^T\right)^{-1} T \tag{9}$$

If the $h(x)$ feature mapping is not known, we can work around it uses the kernel method based on Mercer's condition as suggested by G.B. Huang [43]. The kernel formula is as follows:

$$O = HH^T : m_{ij} = h(x_i)h(x_j) = \Omega(x_i, x_j) \tag{10}$$

The definition of the output function y (x) from the kernel extreme machine learning (K-ELM) is stated as follows:

$$y(x) = [\Omega(x, x_1), \ldots, \Omega(x, x_M)\,] \left(\frac{1}{C_r} + O\right)^{-1} T \tag{11}$$

where $O = HH^T$.

The support vector engine model (SVM) is like Eq. (7) by providing closed-form expressions for kernel coefficients. To check the performance of the ELM learning algorithm, the radial basis function (RBF) is used as the kernel as written in Eq. (12).

$$\Omega(x, y) = exp\left(\frac{\|x - y\|^2}{2\sigma^2}\right) \tag{12}$$

Fig. 4 shows the network structure of the K-ELM algorithm. The parameter selection of the regularization coefficient Cr and the kernel parameter σ must be chosen correctly because it greatly affects K-ELM performance. The stability of the K-ELM learning algorithm is better than the standard ELM. The K-ELM learning algorithm is also faster than SVM.

3. Implementation of proposed method

The K-ELM model utilized in this paper is depicted in Fig. 5. The features chosen as input data of K-ELM consist of the generator real power *P*, reactive power *Q*, terminal voltage V_t, and equivalent reactance X_e. The predicted parameter of PSS including K_{stab}, T_1, and T_2 is the output data of K-ELM. The procedures for adaptive PSS model are classified into two parts that are training phase and testing phase.

The workflow of PSS based on K-ELM for training process is shown in Fig. 6 and described as follows:

1. Collect the data of generator, transmission, and load for SMIB model and PSS model from [44].

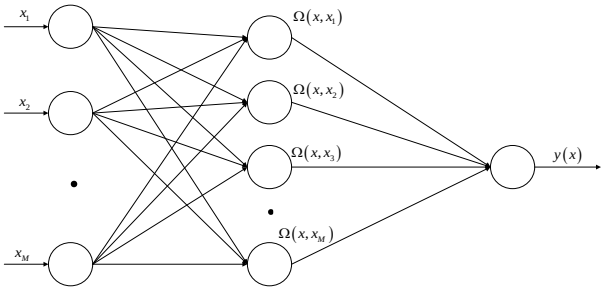

Figure. 4 The scheme of K-ELM algorithm

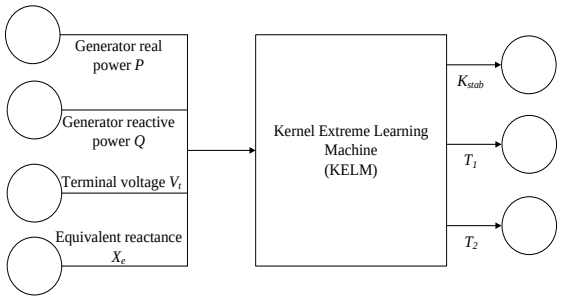

Figure. 5 The proposed K-ELM scheme

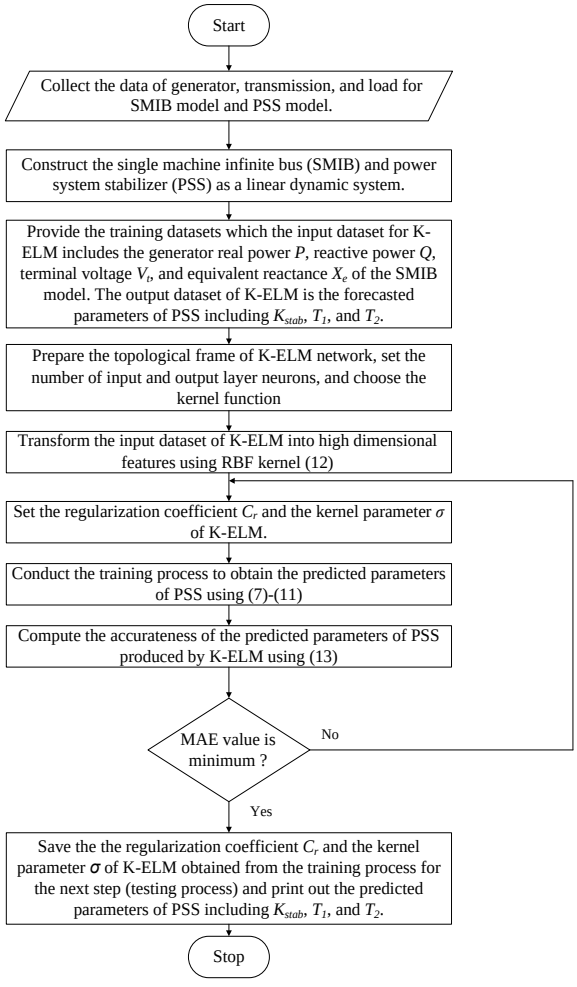

Figure. 6 The workflow of PSS based on KELM for training process

2. Construct the single machine infinite bus (SMIB) and power system stabilizer (PSS) as a linear dynamic system as shown in Figs. 1-2.
3. Provide the training datasets which the input dataset for K-ELM includes the generator real power P, reactive power Q, terminal voltage V_t, and equivalent reactance X_e of the SMIB model. The output dataset of K-ELM is the forecasted parameters of PSS including K_{stab}, T_1, and T_2.
4. Prepare the topological frame of K-ELM network, set the number of input and output layer neurons as shown in Fig. 4, and choose the kernel function in Eq. (12).
5. Transform the input dataset of K-ELM into high dimensional features using RBF kernel using Eq. (12).
6. Set the regularization coefficient C_r and the kernel parameter σ of K-ELM.
7. Conduct the training process using Eqs. (7) - (10).
8. The forecasted parameters of PSS are produced by using Eq. (11).
9. Compute the accurateness of the predicted parameters of PSS produced by K-ELM. Statistical indicator namely mean square error (MSE), mean absolute error (MAE), and sum square error (SSE) are employed for measuring the performance of K-ELM to forecast the parameters of PSS as provided in Eqs. (13)-(15).

$$MSE = \sum_{i=1}^{N} \frac{(\tilde{y}_i - y_i)^2}{N} \tag{13}$$

$$MAE = \sum_{i=1}^{N} \frac{|\tilde{y}_i - y_i|}{N} \tag{14}$$

$$SSE = \sum_{i=1}^{N} (\tilde{y}_i - y_i)^2 \tag{15}$$

10. If the MAE value is minimum, save the the regularization coefficient C_r and the kernel parameter σ of K-ELM obtained from the training process for the next step (testing process) and print out the predicted parameters of PSS including Kstab, T1, and T2. Otherwise, go to step 6 until the minimum value of MAE are obtained.

After the training process has been conducted, the next stage is the testing phase for the K-ELM method to obtain the appropriate parameters of PSS. The workflow of PSS based on K-ELM (KELM-PSS)

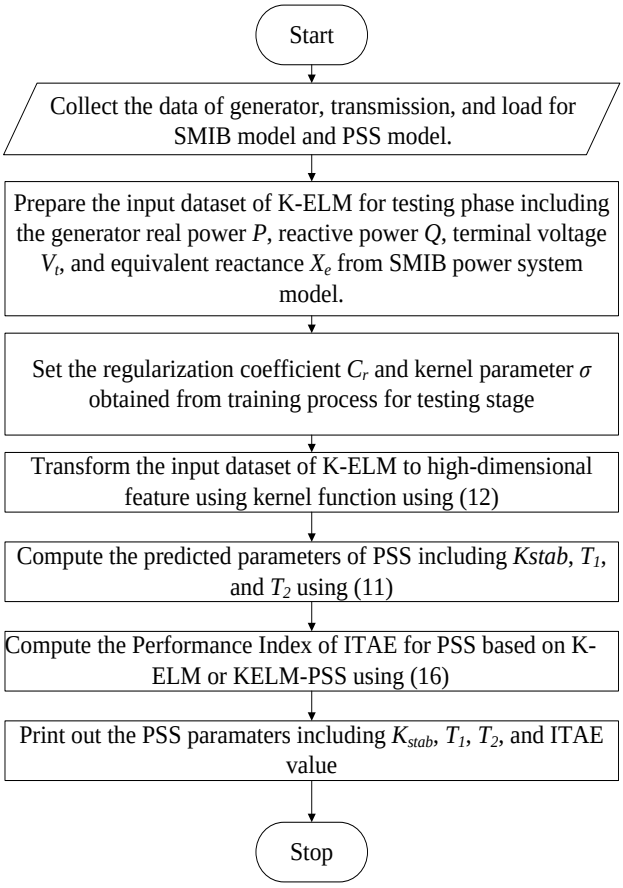

Figure. 7 The workflow of PSS based on KELM for testing phase

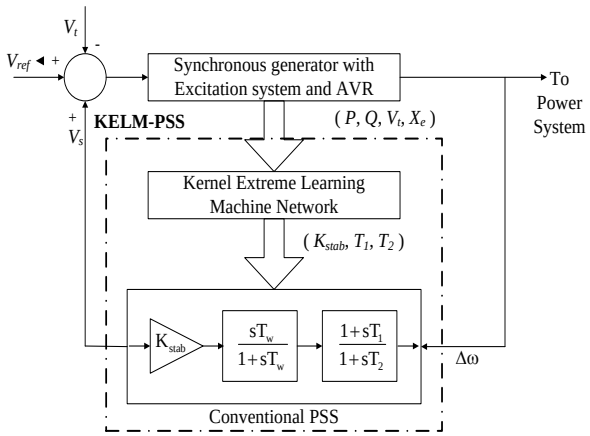

Figure. 8 The schematic diagram of SMIB equipped by KELM-PSS

related to testing stage is described as follows and depicted in Fig. 7.

1. Collect the data of generator, transmission, and load for SMIB model and PSS model from [44].
2. Prepare the input dataset of K-ELM for testing phase including the generator real power P, reactive power Q, terminal voltage V_t, and equivalent reactance X_e from SMIB power system model.
3. Utilize the regularization coefficient C_r and kernel parameter σ of K-ELM for testing stage that has been obtained from training process.
4. Transform the input dataset of K-ELM to high-dimensional feature using kernel function in Eq. (12).
5. Compute the predicted parameters of PSS including K_{stab}, T_1, and T_2 using Eq. (11)
6. Compute the performance index using ITAE for PSS based on K-ELM or KELM-PSS as defined in Eq. (16).

$$ITAE = \int_o^{t_{sim}} t|e(t)|\,dt = \int_o^{t_{sim}} t\left|\Delta\omega_{ref}(t) - \Delta\omega(t)\right|\,dt \quad (16)$$

Every performance index based on integral has certain advantages for control system design. Decrement of system performance index leads to easier and better control system stability. Integral time absolute error (ITAE) is one of the most criterion employed to reduce system error and provide the KELM-PSS values for a desired system response requirement.

7. Print out the PSS parameters (i.e K_{stab}, T_1, and T_2) and ITAE values.

The schematic block diagram of SMIB system model equipped with KELM-PSS is illustrated in Fig. 8. The output dataset of the K-ELM provides the desired PSS parameters (i.e. K_{stab}, T_1, and T_2). The input dataset of the K-ELM network comprises generator real power output (P), reactive power output (Q), terminal voltage (V_t), and equivalent reactance (X_e).

4. Results and discussions

4.1 Data processing

The data of SMIB power system model was collected from [44]. All data were in per unit (p.u), except M or H, and the time constants. M and the time constants were stated in seconds [42]. The datasets utilized for training process was shown in Tables 2 and 3 where the input datasets of K-ELM were generator real power output (P), reactive power output (Q), terminal voltage (V_t), and equivalent reactance (X_e). Therefore, the output datasets of K-ELM were the desired parameters of PSS (i.e. K_{stab}, T_1, and T_2).

The parameters of K-ELM and other machine learning methods (i.e. support vector machine (SVM) [45], least square support vector machine (LS-SVM)

Table 2. The operating condition data of SMIB for training phase

Operating conditions (all values in p.u)			
P	Q	V_t	X_e
0.73	0.07	0.94	0.56
0.97	0.27	0.99	0.55
0.76	0.19	0.95	0.76
0.99	0.23	0.93	0.58
0.85	0.15	0.96	0.56
0.87	0.07	0.91	0.52
0.60	0.22	1.06	0.56
0.86	0.28	0.98	0.71
0.86	0.28	1.02	0.65
0.90	0.19	0.90	0.65

Table 3. The PSS data of SMIB for training phase

PSS parameters		
K_{stab}	T_1	T_2
21.5109	0.3230	0.0556
22.2775	0.2749	0.0667
22.3584	0.4522	0.0862
18.4095	0.3032	0.0771
21.3072	0.4119	0.0818
18.2840	0.2830	0.0587
35.6714	0.2334	0.0577
22.5304	0.3402	0.0760
25.7064	0.2910	0.0670
17.0791	0.3605	0.0839

Table 4. Parameters of SVM, LS-SVM, ELM, and KELM

SVM	LS-SVM	ELM	K-ELM
C = 10	C = 10	Hidden Neuron = 30	C = 10
σ = 0.3	σ = 0.3		σ = 0.3

[46], and extreme learning machine (ELM) methods [47]) utilized in training process and testing phase were illustrated in Table 4.

4.2 Training phase

The main objective of the training process is to obtain the parameters of K-ELM with the minimum MAE value. The best parameters of K-ELM and other machine learning methods obtained from training phase was illustrated in Table 4. Moreover, the datasets utilized for training process were depicted in Tables 2 and 3. The best parameters of PSS obtained by SVM, LS-SVM, ELM, and K-ELM techniques in training process were shown in Tables 5-8.

4.3 Metrics measurement

The most significant results emerged from Tables 9-11 were that the PSS based on K-ELM method could predict the parameters of PSS (i.e. K_{stab}, T_1, T_2). The proposed K-ELM approach could assess the

Table 5. Parameters of PSS obtained by SVM method

SVM-PSS		
K_{stab}	T_1	T_2
21.5933	0.32346	0.05699
22.2911	0.27959	0.06711
22.3762	0.44089	0.08483
18.7703	0.30538	0.07658
21.4078	0.40414	0.08078
18.6685	0.28718	0.0598
34.4795	0.24196	0.05891
22.5668	0.33874	0.07551
25.416	0.29447	0.06742
17.5655	0.35748	0.08275

Table 6. Parameters of PSS obtained by LSSVM technique

LSSVM-PSS		
K_{stab}	T_1	T_2
21.5665	0.32324	0.05646
22.2916	0.27812	0.06697
22.3665	0.44569	0.08541
18.6524	0.30463	0.07674
21.3726	0.4073	0.08122
18.516	0.28543	0.05938
35.0018	0.23818	0.05838
22.5331	0.33912	0.0756
25.5112	0.29323	0.06725
17.3743	0.3587	0.0832

Table 7. Parameters of PSS obtained by ELM approach

ELM-PSS		
K_{stab}	T_1	T_2
21.5112	0.32312	0.05576
22.2761	0.27537	0.06676
22.3562	0.45099	0.08606
18.4393	0.3035	0.07707
21.3022	0.41085	0.08165
18.3249	0.28363	0.05882
35.5414	0.23433	0.05783
22.5442	0.34009	0.07595
25.669	0.29138	0.06706
17.1243	0.36025	0.08380

Table 8. Parameters of PSS obtained by K-ELM method

KELM-PSS		
K_{stab}	T_1	T_2
21.5109	0.323	0.0556
22.2775	0.2749	0.0667
22.3584	0.4522	0.0862
18.4095	0.3032	0.0771
21.3072	0.4119	0.0818
18.284	0.283	0.0587
35.6714	0.2334	0.0577
22.5304	0.3402	0.076
25.7064	0.291	0.067
17.0791	0.3605	0.0839

Table 9. The MSE value

Mean Square Error (MSE)			
SVM-PSS	LSSVM-PSS	ELM-PSS	KELM-PSS
0.067957	0.02314045	0.000771	5.91E-15

Table 10. The MAE value

Mean Absolute Error (MAE)			
SVM-PSS	LSSVM-PSS	ELM-PSS	KELM-PSS
0.1007	0.06048746	0.0104	**5.91E-15**

Table 11. The SSE value

Sum Square Error (SSE)			
SVM-PSS	LSSVM-PSS	ELM-PSS	KELM-PSS
2.0387	0.6942135	0.0231	4.38E-27

Table 12. Computation process time

Central Processing Unit (CPU) Time			
SVMPSS	LSSVMPSS	ELMPSS	KELMPSS
0.3594	0.28125	0.0734	0.00839

parameters of PSS (i.e. K_{stab}, T_1, T_2) as of 5.91E-15 for MSE value, 5.91E-15 for MAE value, and 4.38E-27 for SSE value, respectively. The PSS based on K-ELM method has minimum MSE, MAE, and SSE values, smaller than PSS based on SVM, LS-SVM, and ELM methods. Thus, the performance of the proposed method could minimize error better than other methods in this research work. The CPU time of the proposed method compared to other approaches is shown in Table 12. As shown in Table 12, the best CPU time calculation was resulted by the proposed K-ELM method around 0.00839 second during the training phase; while the computational burden time of SVM, LS-SVM, and ELM techniques were 0.3594 second, 0.28125 second, and 0.0734 second, respectively.

4.4 Testing phase

The best of K-ELM parameters and other approaches obtained from the training process as shown in Table 4 were utilized in the testing phase. In order to evaluate the performances of K-ELM upon changes in the SMIB power system model, a 0.01 p.u. load change has been applied to SMIB power system model as a natural disturbance. Also, the following values of generator real power output P, reactive power output Q, terminal voltage V_t, and equivalent reactance X_e were employed: P = 0.95 p.u, Q = 0.4376 p.u, V_t = 1.0 p.u, and Xe = 0.8 p.u. The comparisons of the proposed approach (KELM-PSS) with other techniques such as CPSS [44], SVM-PSS, LSSVM-PSS, ELM-PSS in order to damp the system oscillation were depicted in Figs. 9 and 10. The overshoot and settling time values in Figs. 9 and 10 were provided in Tables 13-14. To examine the efficacy of the proposed method, ITAE as performance index was considered as depicted in Table 15. To describe the superiority of the proposed method for damping the rotor speed deviation, the overshoot and settling time values as depicted in Fig. 9 and Tables 13 and 14 were analyzed. From Fig. 9 and Table 13, it could be seen that the proposed approach has a rigorously smaller overshoot for rotor speed deviation compared to the other techniques. The proposed method could decrease the overshoot of about 13.08% compared to the CPSS, while the LSSVM-PSS and ELM-PSS could decrease the overshoot around 3.37%, and 9.39%, respectively. SVM-PSS could not well reduce the overshoot of system oscillation compared to CPSS. But SVM-PSS could stabilize the unstable SMIB power system in open loop condition (without PSS).

In terms of settling time values as seen in Fig. 9 and Table 14, the proposed approach could compress the settling time faster than other techniques utilized in this paper as of 4.81 seconds compared to the

Table 13. Overshoot (p.u)

Methods	**$\Delta\omega$**	**$\Delta\delta$**
Without PSS	Unstable	Unstable
CPSS	-0.0001544	-0.01914
SVM-PSS	-0.0001548	-0.01479
LSSVM-PSS	-0.0001492	-0.01638
ELM-PSS	-0.0001399	-0.01773
KELM-PSS	**-0.0001342**	**-0.01735**

Table 14. Settling time (second)

Methods	**$\Delta\omega$**	**$\Delta\delta$**
Without PSS	Unstable	Unstable
CPSS	>5	3.36
SVM-PSS	4.81	2.94
LSSVM-PSS	3.16	2.51
ELM-PSS	2.73	2.31
KELM-PSS	**2.56**	**2.28**

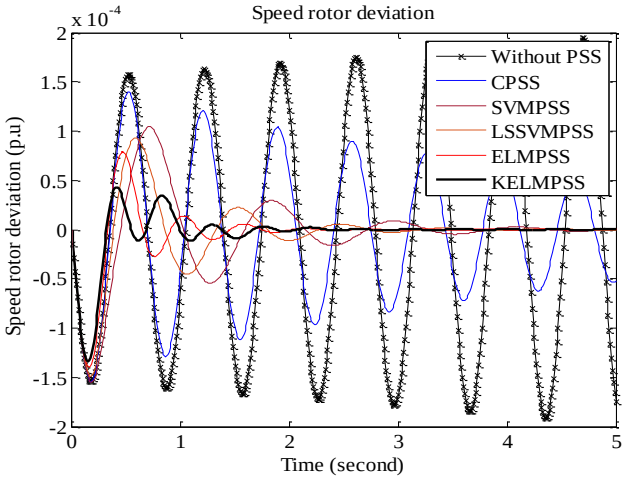

Figure. 9 Speed rotor deviation

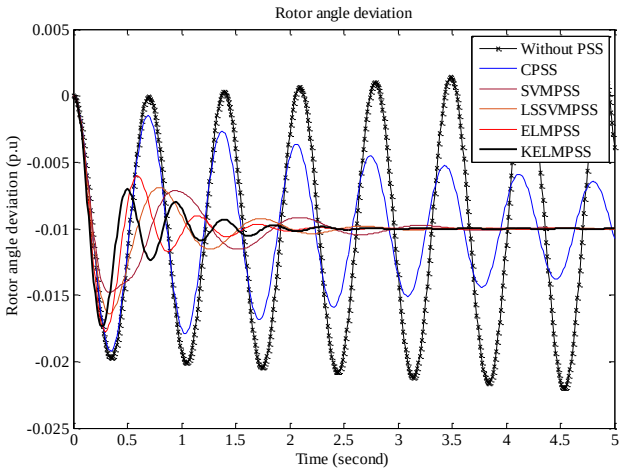

Figure. 10 Rotor angle deviation

Table 15. Performance Index (ITAE value)

PSS based learning method	ITAE Value
Conventional PSS	0.414218
SVM-PSS	0.044893
LSSVM-PSS	0.043046
ELM-PSS	0.043046
ELM-PSS	0.030530
KELM-PSS	**0.024762**

CPSS approach. The proposed technique could bring back the rotor speed to its nominal value about 48.8 % faster than the CPSS technique. While the SVM-PSS, LSSVM-PSS, and ELM-PSS could compress the settling time in 3.8%, 36.8%, and 45.4 % quicker than CPSS method, respectively. In viewpoint of the performance index, the K-ELM method has a smaller value compared to SVM, LSSVM, and ELM methods. From Fig. 9 and Tables 13-15, the proposed method can reduce the overshoot, compress the settling time, and decrease the ITAE values better than SVM, LSSVM, and ELM methods.

When there was changes of load, active power, reactive power, terminal voltage, and equivalent reactance, the rotor angle is also oscillating as is the speed rotor. As seen in Fig. 10 and Tables 13-14, the proposed approach could damp the overshoot of rotor angle about 9.35% and reduce the settling time around 32.14% compared to the CPSS technique. On the contrary, the overshoot of rotor angle could be reduced by the SVM-PSS, LSSVM-PSS, and ELM-PSS techniques as of 22.73%, 14.42%, 7.37% which are better than the CPSS method controller. Additionally, the settling time values that could be achieved by the SVM-PSS, LSSVM-PSS, and ELM-PSS methods were 12.5%, 25.29%, and 31.25% better than the CPSS approach. Although the performance of KELM-PSS is not good to reduce overshoot for rotor angle compared to SVM-PSS and LSSVM-PSS, the proposed method could compress the settling time better than other approaches. In this study, this condition was occurred due to the performance of power system stabilizer (PSS) based on learning algorithm focused to maintain the rotor speed deviation on its nominal value after there was change of operating point on the SMIB system caused by the changes of load, active power, reactive power, terminal voltage, and equivalent reactance values. The proposed method has a good performance in damping of rotor speed deviation and rotor angle deviation where the rotor speed is quickly driven back to their nominal values and rotor angle is rapidly driven towards its new steady-state value; while the system with a CPSS method has the worst performance since it uses a conventional approach to obtain feedback gain to produce signal control injected to excitation system on SMIB. When the control input has a good response, less overshoot, faster settling time, and smaller performance index ITAE, then the response of the SMIB system will be as good as the control input.

5. Conclusions

In this paper, a new approach based on learning algorithm approach in order to adjust automatically the parameters of power system stabilizer has been proposed. The learning algorithm method called kernel extreme learning machine (K-ELM) has been utilized to determine the optimal setting of PSS parameters. In this study, in order to get confidence for the system model of the proposed method, the statistical measures such as MSE, MAE, and SSE were computed for training phase. Moreover, to validate the efficacy of the proposed method in testing stage, the overshoot, settling time, and ITAE were performed to analyse the performance of the proposed method for any changes of load, active power, reactive power, terminal voltage, and equivalent reactance. An increase in the stability of the electric power system through a PSS-based learning algorithm was carried out. The proposed method has a smaller MSE, MAE, and SSE values compared to PSS based on SVM-PSS, LSSVM-PSS, and ELM-PSS in the training phase. Also, the proposed method has a good performance in testing stage by having a smaller overshoot, a faster settling time, and a smaller ITAE value than PSS based on other learning algorithm techniques. This could happened because K-ELM used trained data from the reference paper. Hence, K-ELM can give a more detail and pricise value. Hereafter, the proposed method could increase the performance of dynamic stability for SMIB power system model. For future

work, the development of PSS based on learning algorithm for more realistic systems will be considered. Also, the use of PSS for non-linear power system model for transient stability study will be developed because PSS based on learning algorithm at present is only applied for dynamic stability of SMIB model. Improvement of learning algorithm technique by hybridizing with metaheuristic approach is important subject because the proposed method is not optimized at present.

Conflicts of Interest

The authors declare no conflict of interest.

Author Contributions

Conceptualization, IBG Manuaba and Muhammad Abdillah; methodology, Muhammad Abdillah and Herlambang Setiadi; software, Muhammad Abdillah and Herlambang Setiadi; validation, IBG Manuaba, Muhammad Abdillah and Ramon Zamora; formal analysis, IBG Manuaba and Ramon Zamora; investigation, Ramon Zamora and Herlambang Setiadi; resources, Muhammad Abdillah; writing original draft preparation, IBG Manuaba; writing review and editing, Ramon Zamora and Muhammad Abdillah; visualization, IBG Manuaba, Muhammad Abdillah, and Herlambang Setiadi. All authors have read and agreed to the published version of the manuscript

References

[1] M. K. Deshmukh and C. B. Moorthy, "Review on Stability Analysis of Grid Connected Wind Power Generating System", *International Journal of Electrical and Electronics Engineering Research and Development*, Vol. 3, No. 1, pp. 1–33, 2013.

[2] M. Q. Duong, S. Leva, M. Mussetta, and K. H. Le, "A Comparative Study on Controllers for Improving Transient Stability of DFIG Wind Turbines during Large Disturbances", *Energies*, Vol. 11, No. 1, pp. 480, 2018

[3] A. Xue, J. Zhang, L. Zhang, Y. Sun, J. Cui, and J. Wang, "Transient Frequency Stability Emergency Control for The Power System Interconnected with Offshore Wind Power Through VSC-HVDC", *IEEE Access*, Vol. 8, No. 1, pp. 53133–53140, 2020.

[4] Q. Hui, J. Yang, X. Yang, Z. Chen, Y. Li, and Y. Teng, "A Robust Control Strategy To Improve Transient Stability for AC-DC Interconnected Power System With Wind Farms", *CSEE Journal of Power and Energy Systems*, Vol. 5, No. 1, pp. 259-265, 2019.

[5] M. Abdillah, "Adaptive Hybrid Fuzzy PI-LQR Optimal Control Using Artificial Immune System Via Clonal Selection for Two-Area Load Frequency Control", *International Journal on Electrical Engineering and Informatics*, Vol. 12, pp. 1-19, 2020.

[6] H. Setiadi, N. Mithulananthan, and R. Shah, "Design of Wide-Area POD with Resiliency Using Modified DEA for Power Systems with High Penetration of Renewable Energy", *IET Renewable Power Generation*, Vol. 13, No. 1, pp. 342-351, 2019.

[7] H. Setiadi, N. Mithulananthan, R. Shah, K. Y. Lee, and A.U. Krismanto, "Resilient Wide-Area Multi-Mode Controller Design Based on Bat Algorithm for Power Systems with Renewable Power Generation and Battery Energy Storage Systems", *IET Generation, Transmission & Distribution*, Vol. 3, No. 1, pp. 1884-1894, 2019.

[8] K. R. M. V. Chandrakala and S. Balamurugan, "Adaptive Neuro-Fuzzy Scheduled Load Frequency Controller for Multi-Source Multi-Area System Interconnected via Parallel AC-DC Links", *International Journal on Electrical Engineering and Informatics*, Vol. 10, No. 1, pp. 479-490, 2018.

[9] A. Giannakis, A. Karlis, and L. Y. Karnavas, "A Combined Control Strategy of A DFIG Based on A Sensorless Power Control Through Modified Phase-Locked Loop and Fuzzy Logic Controllers", *Renewable Energy*, Vol. 121, No. 1, pp. 489-501, 2018.

[10] D. Khan, J. A. Ansari, S. A. Khan, and U. Abrar, "Power Optimization Control Scheme for Doubly Fed Induction Generator used in Wind Turbine Generators", *Inventions*, Vol. 5, No. 1, pp. 40, 2020.

[11] N. Masood, Md. N. H. Shazon, H. M. Ahmed, and S. R. Deeba, "Mitigation of Over-Frequency Through Optimal Allocation of BESS in A Low-Inertia Power System", *Energies*, Vol. 13, No. 1, pp. 4555, 2020.

[12] A. G. Zumba, P. F. Córdoba, J. C. Cortés, and V. Mehrmann, "Stability Assessment of Stochastic Differential-Algebraic Systems Via Lyapunov Exponents with An Application To Power Systems", *Mathematics*, Vol. 8, No. 1, pp. 1393, 2020.

[13] A. C. Kathiresan, J. P. Rajan, A. Sivaprakash, T. S. Babu, Md. R. Islam, "An Adaptive Feed-Forward Phase Locked Loop for Grid Synchronization of Renewable Energy

Systems Under Wide Frequency Deviations", *Sustainability*, Vol. 12, No. 1, pp. 7048, 2020.

[14] H. Setiadi and M. Abdillah, "Simultaneous Parameter Tuning of PSS and Wide-Area POD in PV Plant using FPA", *Engineering Journal*, Vol. 23, No. 1, pp. 55-66, 2019.

[15] A. M. Mosaad, M. A. Attia, A. Y. Abdelaziz, "Whale Optimization Algorithm To Tune PID and PIDA Controllers on AVR System", *Ain Shams Engineering Journal*, Vol. 10, No. 1, pp. 755-767, 2019.

[16] J. Bhukya and V. Mahajan, "Optimization Of Damping Controller for PSS And SSSC To Improve Stability of Interconnected System With DFIG Based Wind Farm", *International Journal of Electrical Power & Energy Systems*, Vol. 108, No. 1, pp. 314-335, 2019.

[17] H. Rezaie and M. H. K. Rahbar, "Enhancing Voltage Stability and LVRT Capability of A Wind-Integrated Power System using A Fuzzy-Based SVC", *International Journal of Engineering Science and Technology*, Vol. 22, No. 1, pp. 827-839, 2019.

[18] S. Gurung, F. Jurado, S. Naetiladdanon, and A. Sangswang, "Comparative Analysis of Probabilistic and Deterministic Approach To Tune The Power System Stabilizers using The Directional Bat Algorithm To Improve System Small-Signal Stability", *Electric Power Systems Research*, Vol. 181, No. 1, pp. 106176, 2020.

[19] A. M. Hemeida, M. M. Hamada, Y. A. Mobarak, A. El-Bahnasawy, M. G. Ashmawy, and T. Senjyu, "TCSC with Auxiliary Controls Based Voltage and Reactive Power Controls on Grid Power System", *Ain Shams Engineering Journal*, Vol. 11, No. 1, pp. 587-609, 2020.

[20] B. V. Kumar and V. Ramaiah, "Enhancement of Dynamic Stability By Optimal Location and Capacity of UPFC: A Hybrid Approach", *Energy*, Vol. 190, No. 1, pp. 116464, 2020.

[21] A. Noori, M. J. Shahbazadeh, and M. Eslami, "Designing of Wide-Area Damping Controller For Stability Improvement in A Large-Scale Power System in Presence of Wind Farms and SMES Compensator", *International Journal of Electrical Power & Energy Systems*, Vol. 119, No. 1, pp. 105936, 2020.

[22] S. Asvapoositku and R. Preece, "Impact of HVDC Dynamic Modelling on Power System Small Signal Stability Assessment", *International Journal of Electrical Power & Energy Systems*, Vol. 123, No. 1, pp. 106327, 2020.

[23] V. Kumar, A. S. Pandey, and S. K. Sinha, "Stability Improvement of DFIG-Based Wind Farm Integrated Power System using ANFIS Controlled STATCOM", *Energies*, Vol. 13, No. 1, pp. 4707, 2020.

[24] Y. Liang, Y. He, and Y. Niu, "Microgrid Frequency Fluctuation Attenuation using Improved Fuzzy Adaptive Damping-Based VSG Considering Dynamics and Allowable Deviation", *Energies*, Vol. 13, No. 1, pp. 4885, 2020.

[25] I. Kamwa, R. Grondin, and G. Trudel, "IEEE PSS2B Versus PSS4B: The Limits of Performance of Modern Power System Stabilizers", *IEEE Trans. Power Syst.*, Vol. 20, No. 1, pp. 903–915, 2005.

[26] J. Morsali, R. Kazemzadeh, and M. R. Azizian, "Introducing PID-based PSS2B Stabilizer in Coordination with TCSC Damping Controller to Improve Power System Dynamic Stability", In: *Proc. of 2014 22nd Iranian Conference on Electrical Engineering (ICEE),* Tehran, Iran, pp. 836–841, 2014.

[27] D. Rimorov, I. Kamwa, and G. Joós, "Model-Based Tuning Approach for Multi-Band Power System Stabilisers PSS4B using An Improved Modal Performance Index", *IET Gener. Transm. Distrib.*, Vol. 9, No. 1, pp. 2135–2143, 2015.

[28] A. Yaghooti, M. O. Buygi, and M. H. M. Shanechi, "Designing Coordinated Power System Stabilizers: A Reference Model Based Controller Design", *IEEE Trans. Power Syst.*, Vol. 31, No. 1, pp. 2914–2924, 2016.

[29] H. M. Soliman and H. A. Yousef, "Saturated Robust Power System Stabilizers", *Int. J. Electr. Power Energy Syst.*, Vol. 73, No. 1, pp. 608–614, 2015.

[30] R. You, H. J. Eghbali, and M. H. Nehrir, "An Online Adaptive Neuro-Fuzzy Power System Stabilizer For Multimachine Systems", *IEEE Power Eng. Rev*, Vol. 22, No. 1, pp. 128–135, 2007.

[31] Y. Zhang, G. P. Chen, O. P. Malik, G. S. Hope, "An Artificial Neural Network Based Adaptive Power System Stabilizer", *IEEE Trans. Energy Convers.*, Vol. 8, No. 1, pp. 71–77, 1993.

[32] A. Ghosh, G. Ledwich, O. P. Malik, and G. S. Hope, "Power System Stabilizer Based on Adaptive Control Techniques", *IEEE Trans. Power Appar. Syst*, PAS-103, pp. 1983–1989, 1984.

[33] M. Farahani and S. Ganjefar, "Intelligent Power System Stabilizer Design using Adaptive Fuzzy Sliding Mode Controller",

Neurocomputing, Vol. 226, No. 1, pp. 135-144, 2017.

[34] N. N. Islam, M. A. Hannan, H. Shareef, and A. Mohamed, "An Application of Backtracking Search Algorithm in Designing Power System Stabilizers for Large Multi-Machine System", *Neurocomputing*, Vol. 237, No. 1, pp. 175-184, 2017.

[35] S. Gomes, C. H. C. Guimarães, N. Martins, and G. N. Taranto, "Damped Nyquist Plot for A Pole Placement Design of Power System Stabilizers", *Electric Power Systems Research*, Vol. 158, No. 1, pp. 158-169, 2018.

[36] Md. Shafiullah, Md. J. Rana, Md. S. Alam, and M. A. Abido, "Online Tuning of Power System Stabilizer Employing Genetic Programming for Stability Enhancement", *Journal of Electrical Systems and Information Technology*, Vol. 5, No. 1, pp. 287-299, 2018.

[37] D. Chitara, K. R. Niazi, A. Swarnkar, and N. Gupta, "Cuckoo Search Optimization Algorithm for Designing of A Multimachine Power System Stabilizer", *IEEE Transactions on Industry Applications*, Vol. 54, No. 1, pp. 3056–3065, 2018.

[38] M. Rahmatian and S. Seyedtabaii, "Multi-Machine Optimal Power System Stabilizers Design Based on System Stability And Nonlinearity Indices using Hyper-Spherical Search Method", *International Journal of Electrical Power & Energy Systems*, Vol. 105, No. 1, pp. 729-740, 2019.

[39] S. Ghosh, Y. J. Isbeih, M. S. El Moursi, and E. F. El-Saadany, "Cross-Gramian Model Reduction Approach for Tuning Power System Stabilizers in Large Power Networks", *IEEE Transactions on Power Systems*, Vol. 35, No. 1, pp. 1911–1922, 2020.

[40] H. Verdejo, V. Pino, W. Kliemann, C. Becker, and J. Delpiano, "Implementation of Particle Swarm Optimization (PSO) Algorithm for Tuning of Power System Stabilizers in Multimachine Electric Power Systems", *Energies*, Vol. 13, No. 1, pp. 2093, 2020.

[41] I. B. G. Manuaba, A. Priyadi, and M. H. Purnomo, "Coordination Tuning PID-PSS And TCSC Based Model of Single Machine Infinite Bus using Combination Bacteria Foraging-Particle Swam Optimization Method", *International Review of Electrical Engineering*, Vol. 6, No. 1, pp. 787-794, 2015.

[42] P. Kundur, *Power System Stability and Control*, 1st ed.; McGraw-Hill, Inc.: Toronto, Canada, 1994, pp. 727–766.

[43] G. B. Huang, Q. Y. Zhu, and C. K. Siew, "Extreme Learning Machine: Theory and Applications", *Neurocomputing*, Vol. 70, No. 1, pp. 489-501, 2006.

[44] R. Segal, M. L. Kothari, and S. Madnani, "Radial Basis Function (RBF) Network Adaptive Power System Stabilizer", *IEEE Transactions on Power Systems*, Vol. 15, No. 1, pp. 722-727, 2000.

[45] J. Pahasa and I. Ngamroo, "Adaptive Power System Stabilizer Design Using Optimal Support Vector Machines Based on Harmony Search Algorithm", *Electric Power Components and Systems*, Vol. 42, No. 5, pp. 439-452, 2014.

[46] J. Pahasa and I. Ngamroo, "Least Square Support Vector Machine for Power System Stabilizer Design Using Wide Area Phasor Measurement", *International Journal of Innovative Computing, Information, and Control*, Vol. 7, No. 7(b), pp. 4487-4501, 2011.

[47] Md. Shafiullah, Md. J. Rana, M. S. Shahriar, F.A. Al-Sulaiman, S.D. Ahmed, and A. Ali, "Extreme learning machine for real-time damping of LFO in power system networks", *Electrical Engineering*, Vol. 103, No. 1, pp. 279-292, 2021.